

Contents lists available at [ScienceDirect](http://ScienceDirect)

## Sensing and Bio-Sensing Research

journal homepage: [www.elsevier.com/locate/sbsr](http://www.elsevier.com/locate/sbsr)

# How microelectrode array-based chick forebrain neuron biosensors respond to glutamate NMDA receptor antagonist AP5 and GABA<sub>A</sub> receptor antagonist musimol



Serena Y. Kuang, Xiaoqi Yang, Zhonghai Wang, Ting Huang, Mark Kindy, Tingfei Xi, Bruce Z. Gao \*

Clemson University, 201-3 Rhodes Hall, 29634 Clemson, SC, United States

## ARTICLE INFO

## Article history:

Received 21 January 2016

Accepted 30 June 2016

## Keywords:

Biosensor

Microelectrode array

Neurotoxicity

Chick forebrain neuron

AP5

Musimol

## ABSTRACT

We have established a long-term, stable primary chick forebrain neuron (FBN) culture on a microelectrode array platform as a biosensor system for neurotoxicant screening and for neuroelectrophysiological studies for multiple purposes. This paper reports some of our results, which characterize the biosensor pharmacologically. Dose-response experiments were conducted using NMDA receptor antagonist AP5 and GABA<sub>A</sub> receptor agonist musimol (MUS). The chick FBN biosensor (C-FBN-biosensor) responds to the two agents in a pattern similar to that of rodent counterparts; the estimated EC<sub>50</sub>s (the effective concentration that causes 50% inhibition of the maximal effect) are 2.3 μM and 0.25 μM, respectively. Intercultural and intracultural reproducibility and long-term reusability of the C-FBN-biosensor are addressed and discussed. A phenomenon of sensitization of the biosensor that accompanies intracultural reproducibility in paired dose-response experiments for the same agent (AP5 or MUS) is reported. The potential application of the C-FBN-biosensor as an alternative to rodent biosensors in shared sensing domains (NMDA receptor and GABA<sub>A</sub> receptor) is suggested.

© 2016 The Authors. Published by Elsevier B.V. This is an open access article under the CC BY-NC-ND license (<http://creativecommons.org/licenses/by-nc-nd/4.0/>).

## 1. Introduction

Dissociated animal neurons are able to form a neuronal network within a couple of days after being plated on a microelectrode array (MEA) with adequate density [6,10,11]. The developing neuronal network spikes spontaneously. An MEA can trace this spontaneous spiking activity (SSA), which is actually an extracellular record of action potentials, from the neuronal network cultured on the MEA surface. SSA is subject to various physical and/or chemical changes in the environment, including changes in temperature, osmolarity, and pH of the culture medium [19]; mechanical disturbances [3,9]; and the presence of neuroactive or neurotoxic agents [17]. These environmental changes could cause a change in the rate of SSA and its firing patterns. For this reason, coupling animal neuron culture with MEA technology forms a biosensor system. An MEA-based neuron biosensor is a sensitive functional platform that enables a broad spectrum of research related to the fields of electrophysiology, neuroscience, pharmacology, neurotoxicology, biology, etc. Its value for rapid, sensitive assessment of functional neurotoxicity has drawn increasing attention in recent decades [6].

The most widely investigated and used neuron sources for development of MEA-based neuron biosensor are rodent cortex, hippocampus,

and spinal cord [6]. However, the increasing chemical pollutants in our environment would require millions of animals to screen for neurotoxicants [1,4], making rodent-sourced neurons prohibitively expensive in both time and money. The technology to generate human-induced pluripotent stem cells (hiPSCs) from mature human cell sources [23] has great potential for providing a large supply of human neurons for neurotoxin assessment [21]. However, there are many challenges and costs associated with ensuring a consistent supply of useful hiPSCs, particularly regarding reprogramming efficiency, differentiation reproducibility, and quality control [21]. Recent and anticipated advances are expected to overcome these issues.

Meanwhile, the findings of Dugas-Ford et al. [2] resolved more than a half century of debate about whether cell-type homologies of the mammalian neocortex exist in the brains of birds. The group showed that neocortical cell-type homologies (in particular, the layer IV input neurons and the layer V neuronal output of mammalian neocortex) are conserved from reptiles to mammals. These cells are organized into very different architectures in different species, forming cortical areas in reptiles, nuclei in birds, and cortical layers in mammals. Based on these findings, we hypothesize that despite dramatically different anatomical architectures between mammals and birds, if cortical tissues from the two species were dissociated and their neurons were cultured on MEAs, they would form in vitro neuronal networks that would exhibit some functional similarities due to the presence of the same types of input and output cells.

\* Corresponding author.

E-mail address: [zgao@clemson.edu](mailto:zgao@clemson.edu) (B.Z. Gao).

For all of the reasons above and to determine the applicability of MEA-based neuron biosensors in multiple research fields, we investigated a rarely used, abundant, economical, easily dissected cortical neuron source, chick forebrain. In an effort to develop a chick forebrain neuron (FBN) biosensor on an MEA that is cost-effective, we accomplished the following: 1) assembled the chick FBN biosensor (C-FBN-biosensor) by establishing a long-term, stable chick FBN culture (C-FBN-C) on an MEA and characterized it morphologically, functionally, and developmentally [10,11]; and 2) tested the C-FBN-biosensor by administering several well-known classic neuroactive agents and studying how the sensor responded to these pharmacological interventions, compared our results with reports on rodent counterparts in the literature, and reported preliminary data in a dissertation study [9]. These classic neuroactive agents included *N*-methyl-D-aspartate (NMDA), a prototype agonist of glutamate NMDA receptor; bicuculline (BIC), a specific GABA<sub>A</sub> receptor blocker; magnesium ion (Mg<sup>2+</sup>), a specific glutamate NMDA receptor blocker; tetrodotoxin (TTX), a specific voltage-gated Na<sup>+</sup> channel blocker; verapamil (VER), a specific voltage-gated L-type Ca<sup>2+</sup> channel blocker; (2*R*)-amino-5-phosphonopentanoate (AP5), a specific glutamate NMDA receptor antagonist; and muscimol (MUS), a specific GABA<sub>A</sub> receptor agonist. Among these seven agents, results from AP5 and MUS are reported here with more detailed analysis. The agent-specific dose-response curves for the two agents were obtained, and values of their EC<sub>50</sub> (the effective concentration that causes 50% inhibition of the maximal effect) were estimated and compared with rodent counterparts; the intraculture reproducibility of the C-FBN-biosensor was addressed, and a phenomenon of biosensor sensitization that accompanied the intraculture reproducibility was reported; and the long-term reusability of the C-FBN-biosensor was demonstrated. Interculture reproducibility is discussed.

Unlike hiPSCs, which are cell-type specific, a C-FBN-C is a mix of dissociated chick forebrain tissues mainly containing cortical neurons and glial cells and thus is considered native cortical tissue-specific. Hence, a biosensor made of C-FBN-C is first useful in its own right. It is unique in the abundance of its source of neurons, ease of forebrain dissection, cost-effectiveness, and effectiveness in the experiments we conducted. The terms C-FBN-C and C-FBN-biosensor are used interchangeably in this paper, with the former focusing on the culture and the latter focusing on its biosensing function.

## 2. Materials and methods

### 2.1. Cell culture

MEA preparation, chick forebrain dissection, and dissociation were the same as described in detail in our previous paper [10]. In brief, sterilized MEA chips (MCSMEA-S1-GR, 200/30ir-Ti with internal ground, MCS GmbH, Reutlingen, Germany) were activated using low oxygen plasma treatment (PDC-32G, Harrick) for 2–3 min. After surface activation, the chips were immediately coated with 0.05% polyethylenimine (PEI, P3143, Sigma) at 37 °C overnight. White Leghorn chick forebrains (Embryonic Day 8, 9, or 10 (E8–E10)) were dissected according to Heidemann et al. [5]). Forebrain cells were then trypsinized (0.25% trypsin, T4049, Sigma) for 5–7 min at 37 °C before undergoing a few gentle titrations. The trypsin effect was deactivated by the addition of serum-containing medium, and the cell suspension was centrifuged at 1000 rpm for 5 min. Cell pellets were washed once again using serum-free Medium 199 (M199, M4530, Sigma) supplemented with 2% B27 (17504-044, Gibco) and 1% antibiotic/antimycotic (15240-062, Gibco) and re-suspended in the same medium for plating on MEA chips.

In contrast to our previous method in which dissociated forebrain cells were plated evenly on the whole area of an MEA chip with an inner diameter of 20 mm [10], in this paper, a modified plating method was used to produce a culture in the center of an MEA surface with a diameter of 8 mm, which dramatically reduced the frequency of medium

change for long-term maintenance of a culture. To produce an 8-mm diameter culture, some leftover bits (about 2 mm thick) of polydimethylsiloxane (PDMS) were obtained from a microfabrication. Holes were cut in these PDMS membranes using a Harris Uni-Core™ with 8-mm diameter (Harris US Pat. No. 7093508). A PDMS ring with the desired diameter was then cut using a razor blade and autoclaved. Prior to plating cells, the PEI used to coat the MEA chips was removed, and the chips were washed 4 times using deionized water and dried in a cell culture hood. This drying process was brief: If too long, it may reduce the hydrophilicity that results from surface activation and PEI coating and thus prevent cells from attaching to the MEA surface. When the MEA surface was dry, a PDMS ring was placed in its center (Fig. 1A). Any air between the MEA surface and the PDMS ring was removed by gently pressing the ring using sterilized forceps. Cell suspension was plated within the area restricted by the PDMS ring (Fig. 1B) at a density of 2000 cells/mm<sup>2</sup>. After plating cells as shown in Fig. 1B, the MEA chip was covered with a Teflon® lid (ALAMEA-MEM5, ALA Scientific) and kept in a regular cell culture incubator for about 45 min. After 45 min, when most cells had precipitated to the MEA surface and attached to it, the PDMS ring was gently removed using a sterilized forceps and 1000 µl first-day culture medium (serum-free M199 used for cell plating) was gently placed on the MEA chip. The MEA chips with Teflon lids were placed in 100 mm petri dishes and held in a regular incubator (37 °C, 5% CO<sub>2</sub>, and 95% humidity). The signals of spontaneous spiking activity (SSA) from cultured neuronal networks are very sensitive to osmotic fluctuation, and the Teflon lid, which is permeable to gases but not to water or bacteria [19], helps minimize osmotic fluctuation in the culture medium between medium changes. One day after cell plating, the medium was changed to Neurobasal® medium (NB, 21103-049, Gibco) supplemented with 1% GluMax (35050-061, Gibco), 2% B27 (17504-044, Gibco), 2% fetal bovine serum (FBS, Sigma), and 1% antibiotic/antimycotic (15240-062, Gibco) and kept in the same incubator. Fig. 1C shows a culture at 66 DIV plated in this modified way using the 8-mm PDMS ring.

During the first three weeks, half of the medium in each MEA chip was changed once a week. After three weeks cultures were transferred to a cell culture incubator with the same oxygen supply and humidity, but with reduced CO<sub>2</sub> supply (0.1%), and medium was partially changed once or twice weekly. No glial cell proliferation inhibitor was used; glial cells were co-cultured naturally with FBNs.

### 2.2. MEA recording and data analysis

SSA signals were recorded using MEAs, amplified using an MCS 1060-INV amplifier (MCS GmbH, Reutlingen, Germany), and collected using MC\_Rack software (Version 4.3.0, MCS GmbH, Reutlingen, Germany) at a 25 kHz sampling rate. MC\_Rack extracted spike information simultaneously. A threshold of  $-7$  times the standard deviation (SD) of the mean noise amplitude was set for spike detection in this study. Bursts were defined using the three criteria described in our previous papers [10,11] and detected using NeuroMEA, a MatLab-based program we developed. NeuroMEA also output many other parameters of SSA (such as burst duration, interburst interval, percent of spikes within bursts, interspike interval within bursts, and so on) and created raster plots that showed the time sequence of the spike for each active channel during a designated period of time. An active channel was defined as having five or more spikes per minute.

SSA signals from C-FBN-Cs were monitored frequently (often every other day) during the first three weeks of development. After three weeks, the responsiveness of C-FBN-Cs to selected classic neuroactive agents was tested using a series of dose-response experiments. C-FBN-Cs that had eleven or more active channels were used for dose-response experiments.

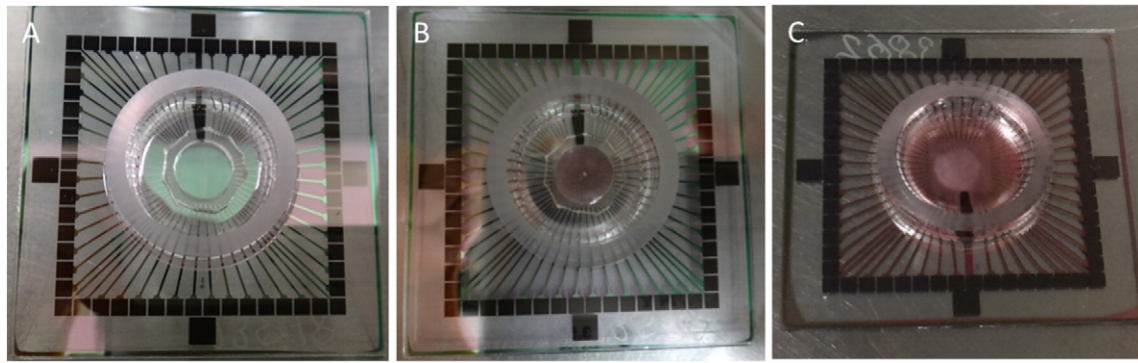


**Fig. 1.** Modified cell plating method using a PDMS ring with desired diameter to restrict the area of cell culture. A: An 8-mm diameter autoclaved PDMS ring in the center of an MEA; B: the cell suspension was restricted to the PDMS ring; and C: a C-FBN-culture plated using this plating method at 66 DIV.

### 2.3. Inhibitory neuroactive agents for conducting dose-response experiment

There are two major categories of neurons in a cortical structure: projection neurons and inter neurons [7,8]. Projection neurons are also called pyramidal cells. Their axons form long bundles of nerve tracts projecting to other (often remote) functional regions of the brain or spinal cord. Pyramidal cells use glutamate as a neurotransmitter. Activation of glutamate receptors excites the target neurons. In contrast, the short axons of inter neurons do not leave the functional region where they are located. Inter neurons are responsible for regulating and synchronizing the firing activities of projection neurons locally in a particular cortical functional region. Most inter neurons use gamma-aminobutyric acid (GABA) as their neurotransmitter, and the activation of GABAergic receptors inhibits the target neurons.

AP5 is a specific antagonist of glutamate *N*-methyl-D-aspartate (NMDA) receptor [15]. When this receptor is blocked by AP5, the excitatory postsynaptic potentials (EPSPs) caused by the natural neurotransmitter glutamate are blocked, and there is little-or-no chance for the postsynaptic neurons to fire action potentials. If the rate of SSA firing is reduced or completely blocked in the presence of AP5 in culture medium, the glutamate NMDA receptor is expressed in C-FBN-C and functioning.

MUS is a specific agonist of GABA<sub>A</sub> receptor [16]. Since the activation of the GABA<sub>A</sub> receptor causes inhibitory postsynaptic potentials (IPSPs), the activation of this receptor has an inhibitory effect on the postsynaptic neurons. If this receptor is expressed and functions in C-FBN-C in the presence of MUS in culture medium, a reduction in or blocking of the firing rate of SSA would be expected.

### 2.4. Dose-response experiment

To know whether and how the SSA signals from C-FBN-C respond to AP5 and MUS, a dose-response curve was obtained for each agent. Stock solutions of both agents were made using phosphate buffered saline (PBS). To determine an appropriate dose range for dose-response experiments,  $\log_{10}[\text{dose}]$  ranges used for rodent counterparts were referenced.

Prior to initial dose administration, a 30-minute recording of SSA signals was performed to obtain baseline reference activity. An initial dose was administered by gently aspirating 90  $\mu\text{l}$  medium from an MEA, mixing it with a dose of agent (less than 10  $\mu\text{l}$ ), then gently sending the mixture back to the MEA and gently rocking it to ensure a fast, even distribution of the added dose. SSA signal recording was started after dose administration and lasted 30 min. Subsequent doses were added in the same way accumulatively, with 30 min of recording after each dose administration. To avoid any perturbation of SSA signals due to dose administration, the last 10 min of each 30-minute recording was used to evaluate the effect of each agent. Immediately after the 30-

minute final dose treatment, the culture was washed three times using fresh medium to remove the neuroactive agent and then recorded for 60 min to trace signal recovery. SSA from most C-FBN-Cs recovered within a 10 to 30 min period after the agent was washed out. Data from C-FBN-Cs that recovered slowly (more than 30 min) were not used in this paper.

### 2.5. Dose-response data process using NeuroMEA

Data obtained from each dose-response experiment was processed using NeuroMEA to plot an initial dose(x)-response(y) curve. The starting point of the curve was the mean burst rate (MBR) of the baseline value averaged from all active channels from one culture. This baseline value was the reference used as a control when no dose was administered. This control value of MBR was set at 1 (100%) on the y-axis. The MBR at each dose was calculated in the same way and was normalized to be a percentage of the control value.

Repeated and reproducible dose-response experiments were done for each agent on different cultures, which generated a group of initial plots for an agent. GraphPad Prism 5 was used to produce a final dose-response curve that is a combination of the group of initial plots (curve fitting).

### 2.6. Sigmoidal curve fitting using GraphPad prism 5

Biologically based dose-response models typically exhibit a sigmoidal shape when the response (on the y-axis) is plotted against the logarithm of the doses (on the x-axis). Each of the selected classic neuroactive agents in this paper has its own agent-specific patterns of sigmoidal curves when applied to rodent cortical neuron networks [14,17,18,20]. We also used the logarithm of the doses ( $\log_{10}[\text{dose}]$ ) to fit the initial curve plots by NeuroMEA to sigmoidal curves. Sigmoid curve fitting is based on the Hill equation [17,25]:

$$Y = \frac{Y_{\text{START}} + (Y_{\text{END}} - Y_{\text{START}})}{(1 + 10^{[\log(\text{EC}_{50}) - \log(X)] \cdot \text{HC}})}$$

where  $y$  is the observed value of a response,  $y_{\text{START}}$  is the highest observed value,  $y_{\text{END}}$  is the lowest observed value at the highest dose,  $\text{EC}_{50}$  is the effective concentration that causes 50% of maximal inhibition, and HC is the Hill coefficient (the slope at the inflection point of the curve, the largest absolute value of the slope of the curve). The larger the absolute value of HC, the steeper the approach to the inflection point [17,25]. Using this model, GraphPad Prism 5 was used for the sigmoidal curve fitting and estimation of the  $\text{EC}_{50}$  value for selected neuroactive agents.



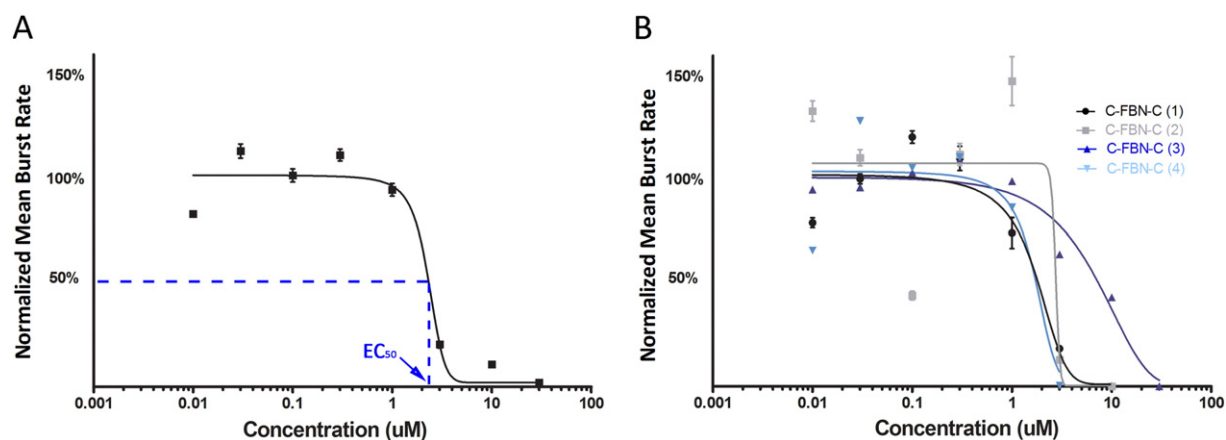


**Fig. 2.** Dose-response curve fitting for AP5. A: A final representative dose-response curve fitted from the four individual dose-response experiments shown in B ( $Y = \text{mean} \pm \text{SE}$ ,  $n = 190$  total active channels from 4 cultures); B: Four initial individual dose-response curves from four individual dose-response experiments conducted on four different cultures.

### 3. Results and discussion

#### 3.1. Dose-response curve fitting for AP5 and MUS

Fig. 2 and Fig. 3 show the curve fittings for AP5 and MUS, respectively.

We consider that the fitted curves for the two agents administered to the C-FBN-Cs (Fig. 2A and Fig. 3A) show representative patterns of the dose-response relationship (agent-specific pattern of sigmoidal dose-response curve). The two figures present the responsive dose range used, initial dose-response curves of each individual dose-response experiment, variations among these initial dose-response curves, and a final representative dose-response curve fitted based on the individual dose-response curves by GraphPad Prism 5 for each agent. These two figures indicate that the glutamate NMDA receptors and GABA<sub>A</sub> receptors are expressed in C-FBN-Cs and respond to AP5 and MUS in a predictable, dose-dependent way.

#### 3.2. An initial comparison between C-FBN-Cs and rodent counterparts in SSA responsiveness to AP5 and MUS

Since the targeted receptors of AP5 and MUS were both expressed and function in C-FBN-Cs, the purpose of this comparison is to explore the possibility and the applicability of using C-FBN-C as an alternative biosensor to rodent counterparts for screening neurotoxicants in shared sensing domains (i.e., shared receptors or ion channels) on the needed

scale and at less cost than rodent biosensors (millions of rodents vs. millions of eggs). To compare the SSA responsiveness between the two species, the following three aspects should be considered: 1) the logarithmic dose range within which a biosensor is reactive to an agent; 2) the  $EC_{50}$ ; and 3) the Hill coefficient (the slope at the inflection point of the curve). The dose ranges were the same or almost the same as the dose ranges we referenced and followed for rodent counterparts. Regarding the Hill coefficient, 1) it was less frequently reported than  $EC_{50}$  in rodent-neuron biosensor research, and 2) we found that the Hill coefficient varied greatly when a broad logarithmic dose range was used to estimate it. For these reasons, values of  $EC_{50}$  only are presented in Table 1 for comparison.

It should be noted that among researchers, experimental settings and animals (chick, rat, and mouse) differed; different (but correlated) variables represented the mean firing rate in dose-response experiments. However, the values of the estimated  $EC_{50}$  for these agents were close in terms of the spread of logarithmic dose ranges used in the experiments. For this reason, this initial comparison suggests that in the two shared sensing domains (NMDA receptor and GABA<sub>A</sub> receptor), C-FBN-Cs respond to their ligands in a similar dose-response pattern, with certain differences in the potency of the two agents as indicated by the comparison of the values of  $EC_{50}$  in Table 1.

For an accurate comparison of the potency of AP5 and MUS between the two species, 1) future dose-response experiments should be conducted with specific focus on the linear segment (the middle segment) of the sigmoid curves within a much narrower dose range than the

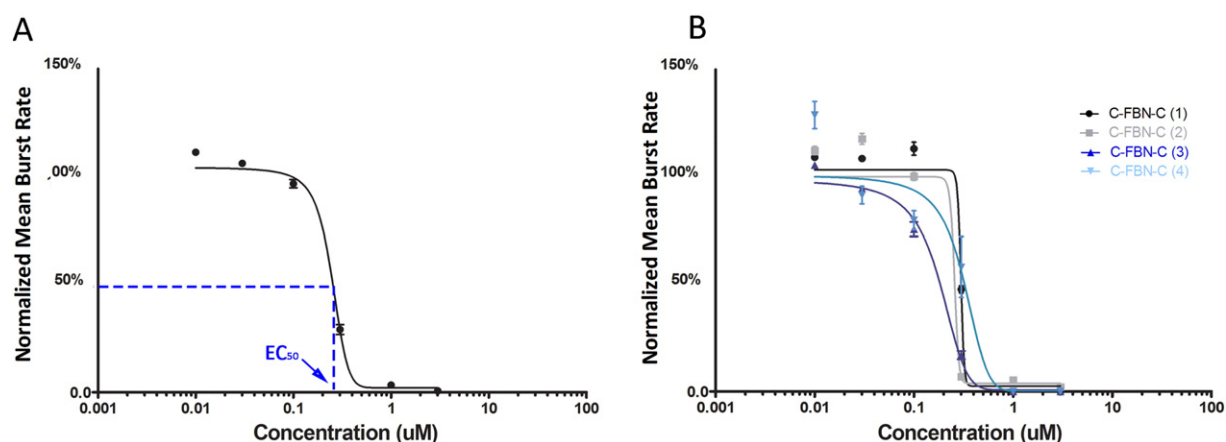


**Fig. 3.** Dose-response curve fitting for MUS. A: A final representative dose-response curve fitted from the four individual dose-response experiments shown in B ( $Y = \text{mean} \pm \text{SE}$ ,  $n = 159$  total active channels from 4 cultures); B: Four initial individual dose-response curves from four individual dose-response experiments conducted on four different cultures.

**Table 1**A comparison of EC<sub>50</sub> between C-FBN-biosensor and rodent counterparts.

Agent	Chick	Rodent	Animal	Neuron	Reference
	EC <sub>50</sub> <sup>a</sup> (μM)	EC <sub>50</sub> <sup>b</sup> (μM)			
AP5	2.3	18	Rats	Cortical	Otto et al. [24])
MUS	0.25	0.16–0.42 <sup>c</sup> 0.03–0.05 <sup>d</sup>	Rats and mice rats	Cortical	Novelino et al. [23]) Scelfo et al. [26])

<sup>a</sup> Mean burst rate (MBR) was used as the mean firing rate (the dependent variable) in dose-response experiments.<sup>b</sup> Mean spike rate (MSR) was used as the mean firing rate (the dependent variable) in dose-response experiments.<sup>c</sup> The range of EC<sub>50</sub> of MUS from six different labs in an interlaboratory reproducibility study.<sup>d</sup> The range of EC<sub>50</sub> of MUS from one lab using different mathematical models.

current logarithmic dose range; 2) additional doses need to be added into this narrower dose range to study the dose-response relationship; and 3) dose-response experiments for the two species need to be conducted in the same experimental setting by the same researcher(s). The EC<sub>50</sub> obtained in this way will better estimate the differences in the potencies of the two agents between the two species; Hill coefficients will also be less variable and become comparable in this context. Other differences between the two species remain unknown.

### 3.3. Intraculture reproducibility and sensitization of the biosensor

Since the inhibitory effects of AP5 and MUS on SSA are both immediate and reversible, and C-FBN-Cs can be maintained with functional stability for several months [10], theoretically, as long as there is no defect or other problem in their receptors or with the cultures, similar patterns of dose-response curve for a particular agent should be reproducible in the same C-FBN-C (intraculture reproducibility). We observed this predicted intraculture reproducibility (Fig. 4). Moreover, when a similar pattern of dose-response relationship was reproduced in paired dose-experiments in the same culture with a 4-to-6-day interexperiment interval, it was accompanied by a leftward shift of the second curve. This left-forward shift occurred not only for AP5 and MUS, it was also observed with other neuroactive agents in our experiments and was quite consistent. Fig. 3 shows examples of the leftward shift of the dose-response curves for AP5 (Fig. 4A) and MUS (Fig. 4B) respectively.

The phenomenon of the leftward shift indicates that when the same agent was administered to the culture the second time, fewer doses were needed to produce an effect of equal magnitude, suggesting a sensitization of the C-FBN-biosensor to the same agent it encountered 4 to 6 days ago. Fig. 4, A and B, show that the leftward shifts of the second curves are less than 10 μM in general. We do not know whether or not this difference is significant as a meaningful sensitization. It is possible that rodent counterparts may also be sensitized by paired use of an

agent, but we have not seen such a report. In the research area of drug abuse, sensitization is a mechanism underlying drug addiction that may take place at various levels of an organism, such as the behavioral level or receptor level [22,24]. Although the mechanisms of sensitization remain poorly understood, at the receptor level it is likely related to long-term potentiation (LTP). LTP is a mechanism underlying synaptic plasticity, which is the ability of chemical synapses to change their strength [13]. More experiments need to be done to better characterize the phenomenon and to see how long it lasts, whether it occurs with longer interexperiment intervals, or whether it still occurs after administration of an agent more than three times. In terms of C-FBN-biosensor development, sensitization seems a desirable property because it increases the biosensor's sensitivity. It should be noted that the initial curves used for curve fitting in Figs. 1 and 2 were all curves obtained when an agent was first administered to the culture.

### 3.4. Long-term intraculture reusability

Table 2 shows the age (days in vitro, DIV) of each C-FBN-C used for experiments described in Figs. 2 and 3, and the number of active channels (active channel count, ACC) for each C-FBN-C on the day the dose-response experiment was conducted.

The range of ages of C-FBN-Cs used in this paper varied widely, from 34 DIV to 112 DIV (Table 2). For all C-FBN-Cs after each dose-response experiment, an agent was washed out immediately, and the SSA was allowed to recover. If the SSA from a culture failed to recover or recovered slowly (longer than 30 min), its dose-response data were not used; and the culture was discarded. If the SSA recovered within 30 min, the culture was reused within at least 4 days after the previous use and a different agent was administered, such as Mg<sup>2+</sup>, TTX, VER, NMDA, or BIC. Table 2 reflects the long-term functional stability and reusability of C-FBN-C as a useful novel biosensor. Although the neuroactive agents we used have immediate and reversible effects on SSA, and

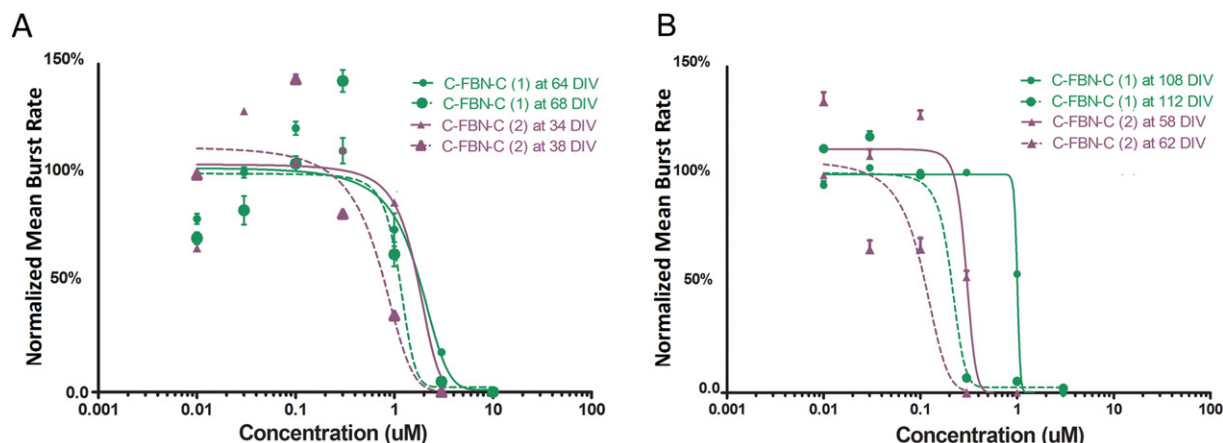


**Fig. 4.** Intraculture reproducibility and sensitization of C-FBN-biosensor to AP5 (A) and MUS (B). A: Paired AP5 dose-response curves were obtained from Culture One (green) and Culture Two (purple) with a 4-day interexperiment interval. Solid lines show the initial dose-response curves, and dashed lines show the second curves, which shifted to the left of the initial ones. B: MUS dose-response curves conducted on two cultures in the same way as on AP5 are shown in A.

**Table 2**

The ages (days in vitro, DIV) of each C-FBN-C used for Figs. 1 and 2 and the active channel count (ACC, the number of active channels) of each sensor on the day of the dose-response experiment.

AP5	DIV	ACC	ACC% <sup>a</sup>	MUS	DIV	ACC	ACC% <sup>a</sup>
Culture_1	64	51	86.4%	Culture_1	96	56	95.0%
Culture_2	37	37	62.7%	Culture_2	112	48	81.4%
Culture_3	93	43	72.9%	Culture_3	43	38	64.4%
Culture_4	34	59	100.0%	Culture_4	36	17	28.8%
<b>Total ACC:</b>		<b>190</b>				<b>159</b>	

<sup>a</sup> ACC%: percent of ACC in total channel count of 59 (the total count of microelectrodes for an MEA used in this paper is 60; 59 are measuring and 1 is the reference).

the interexperiment interval for a sensor to be reused was 4 to 6 days, different receptors or ion channels in a culture were activated or blocked for different time ranges. We do not know whether a previously used agent might have any residual effects that are undetectable within the scale of our measurement. Likewise, we do not know whether such an agent could cause any up- or down-regulation of any receptors or potentiate or reduce the effects of the agent used subsequently.

Potentially, all these elements could have increased the variations of the dose-response experiments, as shown in Fig. 2B and Fig. 3B. In consideration of this and in combination with our results with  $Mg^{2+}$ , TTX, and VER ([12], in review), C-FBN-biosensors still demonstrated remarkable long-term intraculture reusability. In addition, Table 2 also shows a high ACC% in most C-FBN-Cs, reflecting that the C-FBN-Cs were well developed in their environment. The longevity, denser distribution of active channels, and characterizable responsiveness to neuroactive agents show the quality of C-FBN-C as a novel type of animal neuron-based biosensor.

#### 4. Conclusion

Our previous publications have established a five month-long stable C-FBN-C on a microelectrical array as a C-FBN-biosensor [10,11] and characterized it pharmacologically by investigating its responsiveness to  $Mg^{2+}$ , TTX, and VER ([12], in review). This paper presents further pharmacological characterization of the biosensor using AP5 and MUS. The following conclusions can be made: 1) The C-FBN-biosensor responds to AP5 and MUS with a predictable dose-dependent inhibition that is similar to the patterns of rodent counterparts with  $ED_{50}$  of 2.3  $\mu M$  and 0.25  $\mu M$ , respectively; 2) the C-FBN-biosensor shows intrasensor reproducibility and can be sensitized when it is exposed to the same agent again after a few days; 3) the C-FBN-biosensor demonstrates long-term stability and reusability; and 4) the C-FBN-biosensor may be used as an alternative biosensor to rodent counterparts in the shared sensing domains of NMDA receptor and GABA<sub>A</sub> receptor.

#### Acknowledgments

This work was partially supported by funding from the National Institutes of Health through SC COBRE (P20RR021949), the National Natural Science Foundation of China (No. 31070847 and 31370956), the Strategic New Industry Development Special Foundation of Shenzhen (No. JCYJ20130402172114948), and Guangdong Provincial Department of Science and Technology, China (2011B050400011).

#### References

- [1] A.K. Bal-Price, C. Sunol, D.G. Weiss, E. van Vliet, R.H. Westerink, L.G. Costa, *Neurotoxicology* 29 (3) (2008) 520–531, <http://dx.doi.org/10.1016/j.neuro.2008.02.008>.
- [2] J. Dugas-Ford, J.J. Rowell, C.W. Ragsdale, P. Natl. Acad. Sci. USA 9 (2012) 16974–16979, <http://dx.doi.org/10.1073/pnas.1204773109>.
- [3] C.M. Hales, J.D. Rolston, S.M. Potter, J. Visual. Exp. (2010) 30(39), <http://dx.doi.org/10.3791/2056>.
- [4] T. Hartung, S. Bremer, S. Casati, S. Coecke, R. Corvi, S. Fortaner, L. Gribaldo, M. Halder, A.J. Roi, P. Prieto, E. Sabbioni, A. Worth, V. Zuang, *ATLA* 31 (5) (2003) 473–481.
- [5] S.R. Heidemann, M. Reynolds, K. Ngo, P. Lamoureux, *Meth. Cell. Bio.* 71 (2003) 51–65.
- [6] A.F. Johnstone, G.W. Gross, D.G. Weiss, O.H. Schroeder, A. Gramowski, T.J. Shafer, *Neurotoxicology* 31 (2010) 331–350, <http://dx.doi.org/10.1016/j.neuro.2010.04.001>.
- [7] E.R. Kandel, J.H. Schwartz, T.M. Jessell (Eds.), Part I: The Neurobiology of Behavior, in: *Principles of Neural Science*, McGraw-Hill Medical, New York, NY 2000, pp. 5–65.
- [8] E.R. Kandel, J.H. Schwartz, T.M. Jessell (Eds.), Part III: Elementary Interactions between Neurons: Synaptic Transmission, in: *Principles of Neural Science* (p. 212), McGraw-Hill Medical, New York, NY, 2000.
- [9] S.Y. Kuang, Development and Characterization of Chick Forebrain Neuron-Based Neurotoxin Biosensor on a Microelectrode Array [Dissertation], Clemson University, South Carolina, USA, 2014.
- [10] S.Y. Kuang, T. Huang, Z. Wang, Y. Lin, M. Kindy, T. Xi, B.Z. Gao, *RSC Adv.* 5 (2015) 56244–56254, <http://dx.doi.org/10.1039/c5ra09663d>.
- [11] S.Y. Kuang, Z. Wang, T. Huang, L. Wei, T. Xi, M. Kindy, B.Z. Gao, *Biotechnol. Lett.* 37 (2015) 499–509, <http://dx.doi.org/10.1007/s10529-014-1704-1>.
- [12] S.Y. Kuang, X.Q. Yang, T. Huang, Z. Wang, M. Kindy, T. Xi, B.Z. Gao, *NeuroToxicity*, 2016 (in review).
- [13] S. Maren, M. Baudry, *Neurobiol. Learn. Mem.* 63 (1) (1995) 1–18.
- [14] E.R. McConnell, M.A. McClain, J. Ross, W.R. LeFevre, T.J. Shafer, *Neurotoxicology* 33 (5) (2012) 1048–1057, <http://dx.doi.org/10.1016/j.neuro.2012.05.001>.
- [15] R.G. Morris, *J. Neurosci.* 9 (9) (1989) 3040–3057.
- [16] S.R. Naik, A. Guidotti, E. Costa, *Neuropharmacology* 15 (8) (1976) 479–484.
- [17] A. Novellino, B. Scelfo, T. Palosaari, A. Price, T. Sobanski, T.J. Shafer, A.F. Johnstone, G.W. Gross, A. Gramowski, O. Schroeder, K. Jugelt, M. Chiappalone, F. Benfenati, S. Martinoia, M.T. Tedesco, E. Defranchi, P. D'Angelo, M. Whelan, *Front. Neuroengineering* 4 (4) (2011) 1–14, <http://dx.doi.org/10.3389/fneng.2011.00004>.
- [18] F. Otto, P. Götz, W. Fleischer, M. Siebler, *J. Neurosci. Meth.* 128 (1–2) (2003) 173–181.
- [19] S.M. Potter, T.B. DeMarse, *J. Neurosci. Meth.* 110 (1–2) (2001) 17–24.
- [20] B. Scelfo, M. Politi, F. Reniero, T. Palosaari, M. Whelan, J.M. Zaldivar, *Toxicology* 299 (2012) 172–183, <http://dx.doi.org/10.1016/j.tox.2012.05.020>.
- [21] C.W. Scott, M.F. Peters, Y.P. Dragan, *Toxicol. Lett.* 219 (2013) 49–58, <http://dx.doi.org/10.1016/j.toxlet.2013.02.020>.
- [22] J.D. Steketee, *Crit. Rev. Neurobiol.* 17 (2) (2005) 69–86.
- [23] K. Takahashi, K. Tanabe, M. Ohnuki, M. Narita, T. Ichisaka, K. Tomoda, S. Yamanaka, *Cell* 131 (2007) 861–872, <http://dx.doi.org/10.1016/j.cell.2007.11.019>.
- [24] E. Valjent, J. Bertran-Gonzalez, B. Aubier, P. Greengard, D. Hervé, J.A. Girault, *Neuropsychopharmacology* 35 (2) (2010) 401–415, <http://dx.doi.org/10.1038/npp.2009.143>.
- [25] D.G. Weiss, *Neurotoxicity assessment by recording electrical activity from neuronal networks on microelectrode array neurochips*, in: M. Aschner, C. Sunol, A. Bal-Price (Eds.), *Cell Culture Techniques*, Humana Press, New York, NY 2011, pp. 467–480.